https://doi.org/10.5194/egusphere-2023-698
Preprint. Discussion started: 18 April 2023

Arithmetic relationships in Earth's global mean energy flow system

Miklos Zagoni[1]

[1]Eotvos Lorand University, Budapest, 1088, Hungary

Correspondence to: Miklos Zagoni (miklos,zagoni@t-online.hu)

Abstract. Definite ratios and arithmetic relationships can be revealed in Earth's global mean energy flow system. These ratios are not dataset-specific; they can be found in each global energy budget estimate published in the past decade. In this technical paper we point out these arithmetic structures in assessments based on direct observations and climate models; in global energy and water cycle studies; updated energy budget estimates, several satellite-based data products; up to the most recent quantification of the energy flows in the up-to-date global energy and water exchange (GEWEX) data records. The ratios and the corresponding relationships can be recognized both in the all-sky and clear-sky fluxes, and both for radiative (shortwave as well as longwave) and non-radiative energy flow components in the annual global mean. The accuracy of the found relationships allows us to investigate their physical basis, which is identified in known radiation transfer equations. The proposed equations apply only on a subset of the observationally valid arithmetic ratios; other components, having the same accuracy, remain yet unexplained and are presented here only on empirical grounds.

1 Introduction

The 'golden decade' of global energy budgets started when the first reliable global energy balance estimates from space-born active-sounding measurements became available (Wild 2012, Stevens and Schwartz 2012, Stephens et al. 2012). Fundamental changes were proposed in the energy flow components relative to the previously accepted depictions (Kiehl and Trenberth 1997, Trenberth et al. 2009) as first described by Wild (2012), where the top-of-atmosphere (TOA), within-atmosphere, and surface fluxes gained their recent magnitudes after sizeable modifications; the largest shift was made in Back Radiation (downward longwave radiation, DLR), which was increased by 20 Wm^{-2} from its previous 'ad hoc' estimate of 324 Wm^{-2}.

One of the earliest energy balance distributions that displayed uncertainties was Stevens and Schwartz (2012). A simple look on that diagram reveals an unexpected numerical fact: using the value of the longwave cloud radiative effect (LWCRE) from that study (borrowed from CERES, Wielicki et. al. 1996) of 26.5 Wm^{-2} as a unit flux, the other flux components in the diagram can be expressed as integer multiples of this unit, within the stated range of uncertainty (see Figure 1). The only exception at the surface is solar absorption which has a slightly lower integer multiple position value (159 Wm^{-2}, instead of falling into the range of 161-168 Wm^{-2}). It accepted the lower TSI value of 1360.8 ± 0.5 Wm^{-2} (Kopp and Lean 2011).

https://doi.org/10.5194/egusphere-2023-698
Preprint. Discussion started: 18 April 2023

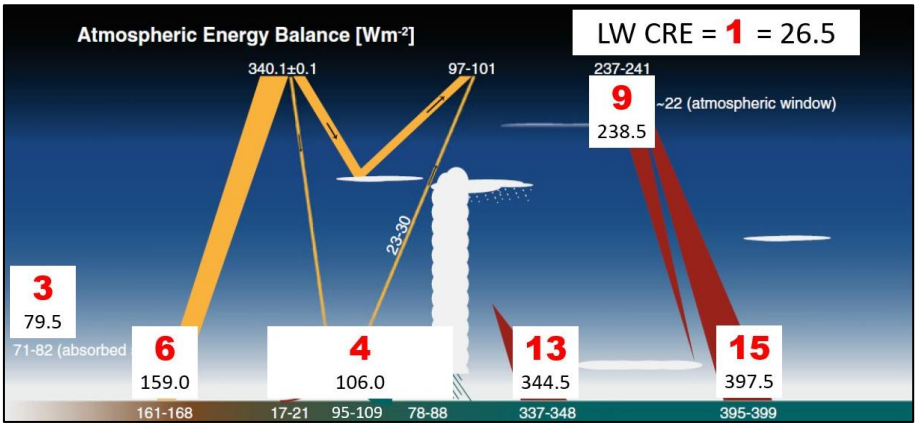

Figure 1: Earth's global and annual mean energy flow system. Values are presented as a two-sigma range (Wm^{-2}). Original: Stevens and Schwartz (2012). LW CRE is inserted from their study, with the value from CERES EBAF. Numbers in red bold typeface are expressed in the unit of 26.5 Wm^{-2}.

The accuracy is remarkable: no such relationships were expected or described in any of the published studies. To decide whether they are coincidences or have physical basis, we had a look on other published global energy budget estimates of that time. We found the same ratios in another updated energy balance estimate (Stephens et al. 2012); the novelty of this graphical representation is the explicit expression of clear-sky fluxes and the longwave cloud effect (LWCRE), both at the top-of-atmosphere (TOA) and at the surface (SFC). A part of the original diagram is shown in Figure 2.

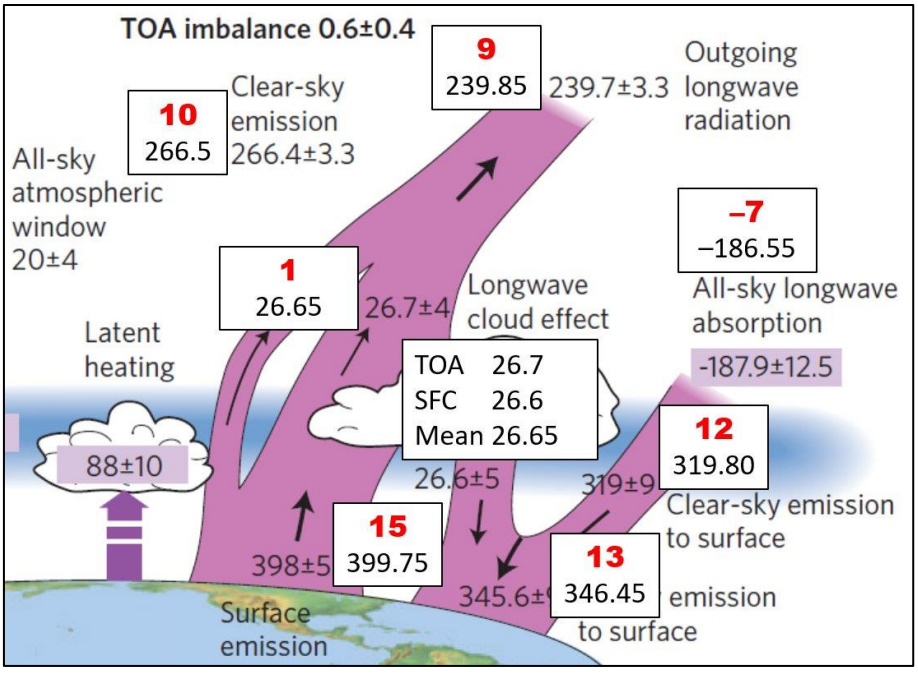

Figure 2: Part of the updated energy balance diagram of Stephens et al. (2012), with integer ratios and a specific equation. Differences of the integer position from their given value are also indicated.

https://doi.org/10.5194/egusphere-2023-698
Preprint. Discussion started: 18 April 2023

Accuracy at TOA is 0.1 Wm^{-2} in clear-sky emission and 0.15 Wm^{-2} in all-sky emission. The difference in the clear-sky emission from the atmosphere to the surface is 0.8 Wm^{-2}, and in the all-sky emission 0.85 Wm^{-2}. The largest difference from the integer position in the longwave is in the flux component of surface emission (1.75 Wm^{-2}, still far within the stated ±5 Wm^{-2} uncertainty. A further observation is that the flux component of all-sky emission to surface (downward longwave radiation, DLR = 345.6 Wm^{-2}), and all-sky longwave absorption (-187.9 Wm^{-2}), together, contain the energy of twice the clear-sky emission to space (clear-sky OLR = 266.4 Wm^{-2}), including the TOA imbalance (0.6 Wm^{-2}), with an extremely small difference of 0.1 Wm^{-2}. This equality, if does not appear by chance but valid in general, would cast a strict constraint on the magnitude atmospheric longwave absorption and emission processes, connecting them to twice the clear-sky OLR.

One year later the IPCC published its Fifth Assessment Report, where Figure 2.11 (based on Wild et al. 2013) provides us with another update of the global mean energy budget, including data from satellites, surface observations and climate models. It is an all-sky assessment with no LWCRE, so to control the integer ratio system we take LWCRE value from the Stephens et al. (2012) diagram as 26.67 Wm^{-2} as unit one. The solar fluxes have exact integer positions at the TOA (on the cross-section disk to incoming solar radiation, before division by 4 for spherical weighting); at the surface the largest difference is in thermal downward radiation, 4.7 Wm^{-2}, still in the magnitude of the CERES instrument calibration uncertainty (see Figure 3).

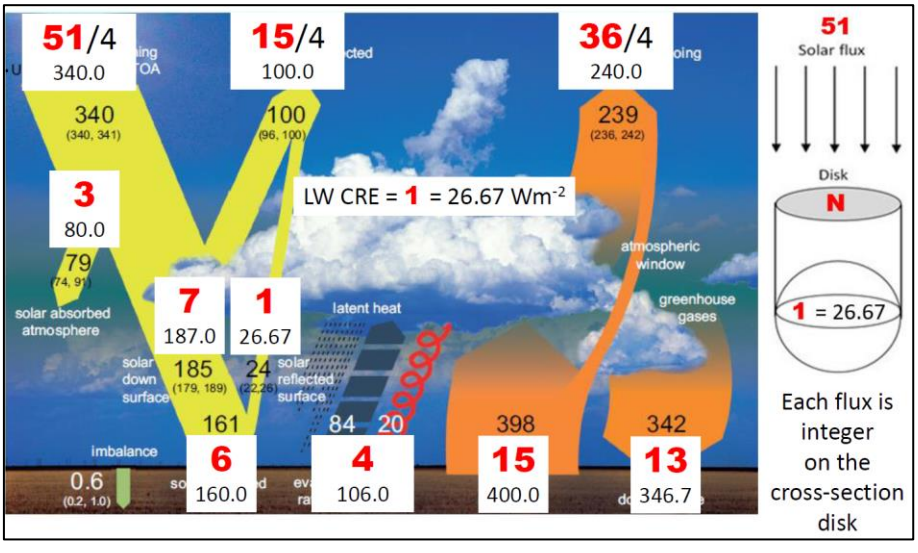

Figure 3: Global mean energy budget from IPCC (2013, Fig. 2.11), with our projection of the integer ratios. The largest difference is 4.7 Wm^{-2} thermal down surface, still in the magnitude of CERES observation uncertainty.

These arithmetic ratios and regularities call for interpretation, but first let us check them on other energy budget estimates. Loeb (2014) gives the values based exclusively on CERES observations (Figure 4).

https://doi.org/10.5194/egusphere-2023-698
Preprint. Discussion started: 18 April 2023

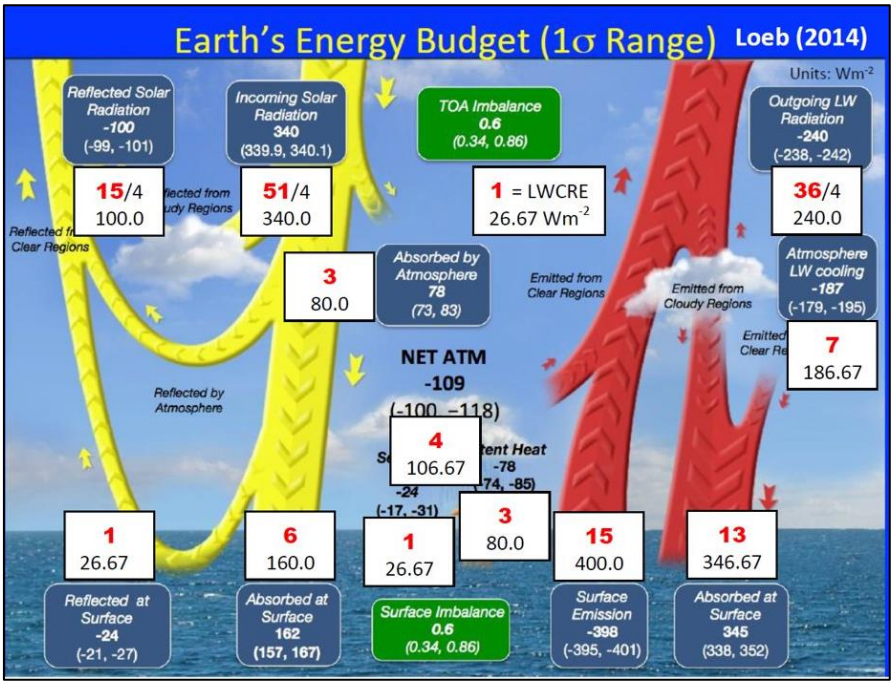

Figure 4: Data in the diagram (Loeb 2014), based on CERES EBAF Edition 2.8. We take LWCRE from the same data product. Fluxes from the integer ratios agree within the given uncertainty for all flux components.

NASA Energy and Water-cycle Study (NEWS, L'Ecuyer et al. (2015) performed a joint assessment of the energy and water fluxes, presented in an optimized global energy budget distribution. Stephens and L'Ecuyer (2015) updated the data in a second-optimization process, constraining surface flues more tightly to CERES observations. Latent heat and sensible heat (evaporation) components of the convective flux are separated (Figure 5). Their accurate fit into integer positions (with a difference of -0.68 Wm^{-2} in sensible heat and 1.94 Wm^{-2} in evaporation), if does not happen by chance, calls for explanation.

From a historical point of view, this was the first estimate where we found internal relationships within the data. The two arithmetic equations presented in Figure 5 connect surface fluxes directly to TOA fluxes (including LWCRE), for all-sky conditions. We show their deduction from Schwarzschild's radiative transfer equation in Section 3; their validation on different data products is presented in Section 4. Integer solution of the equations is given in Section 5.

https://doi.org/10.5194/egusphere-2023-698
Preprint. Discussion started: 18 April 2023

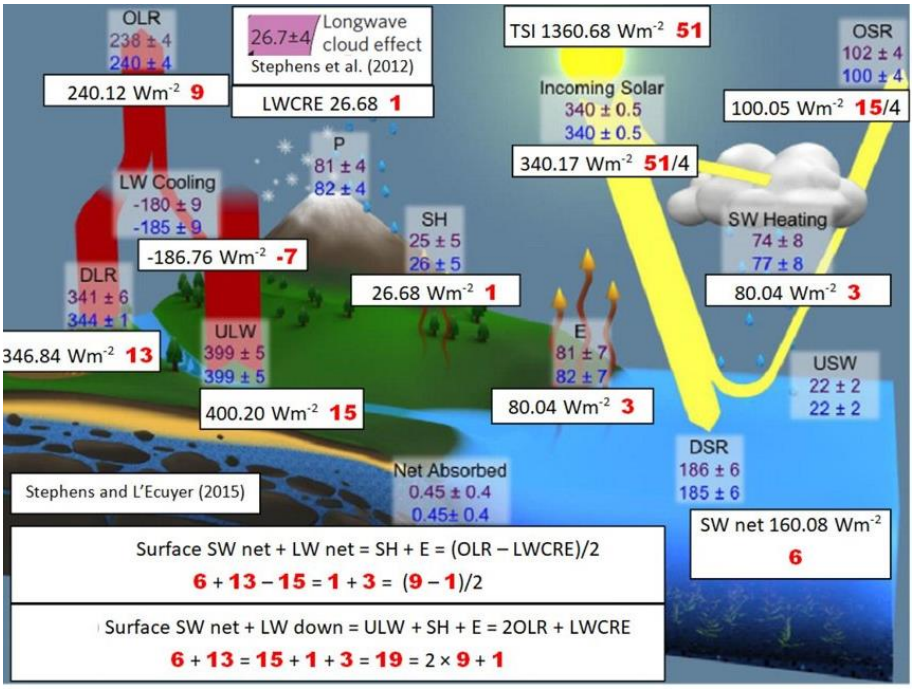

Figure 5: Global mean energy budget from Stephens and L'Ecuyer (2015), based on L'Ecuyer et al. (2015), after application of relevant energy and water cycle balance constraints and a second-optimization to constrain surface fluxes to CERES observations; with our additions (integers, their value in Wm^{-2}, and two relationships. LWCRE = 26.68 Wm^{-2} is close to the value of 26.7 Wm^{-2} given in a contemporary study (Stephens et al. 2012).

Let us call attention to the value of LWCRE = 26.68 Wm^{-2}, giving total solar irradiance TSI = 1360.68 Wm^{-2}, identical to 51 units in the integer system.

Figure 6 and Figure 7 show the energy budget from the latest IPCC AR6 (2021) report for all-sky and clear-sky case.

https://doi.org/10.5194/egusphere-2023-698
Preprint. Discussion started: 18 April 2023

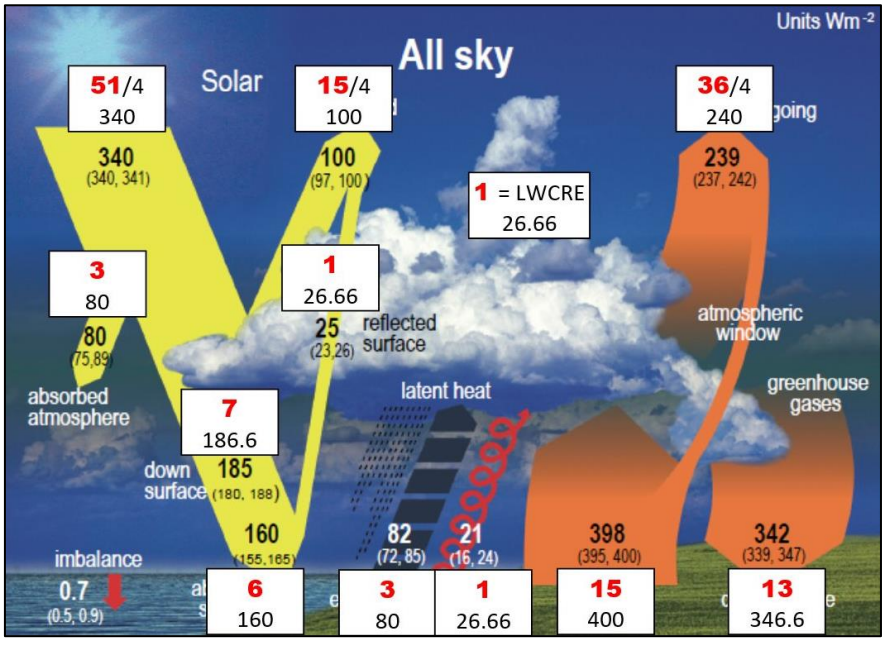

Figure 6: IPCC AR6 (2021, Figure 7.2) global mean energy budget from Wild et al. (2015, 2018), with the integer positions. SW at TOA, in-atmosphere and at the surface are exact, largest difference is in LW down surface. Notice that the most recent edition of CERES EBAF Ed4.2 (2023) gives 346.1 Wm^{-2} for this flux component.

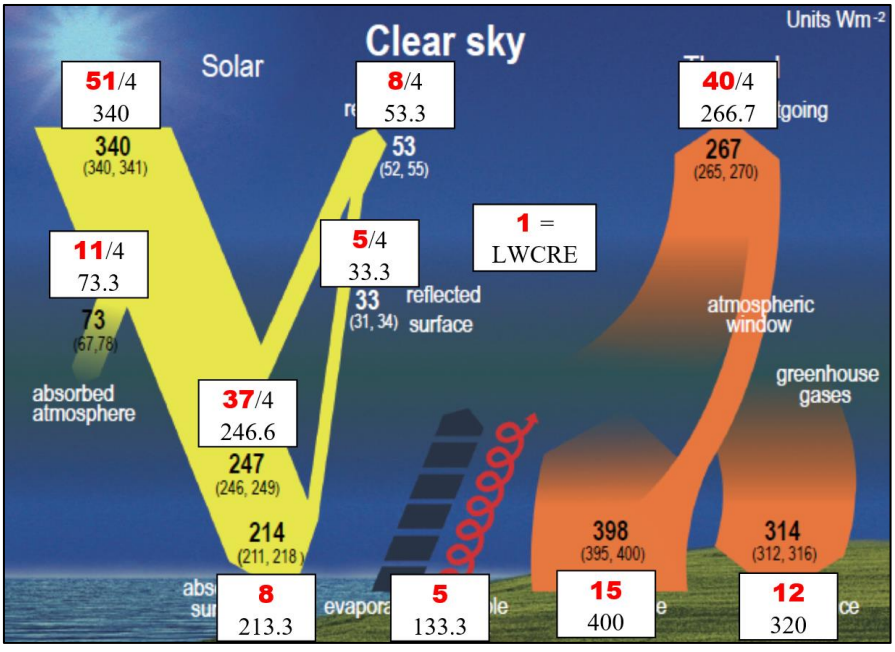

Figure 7: As in Figure 6, for clear-sky case. TOA fluxes are exact; SW atmosphere and surface are precise; the largest difference is in LW down surface. Notice that CERES EBAF Ed4.2 gives 317.86 Wm^{-2} for this value.

https://doi.org/10.5194/egusphere-2023-698
Preprint. Discussion started: 18 April 2023

2 Data

The first global energy balance based on reliable CERES data was Stevens and Schwartz (2012); data from Table 1 is used in our Table 1, first column). When our study has started, only CERES EBAF Edition 2.8 was available with 16 years of observations (Table I, second column). The latest available update to the CERES data is Edition 4.1 (Loeb et al. 2018; Kato et al. 2018) Version 3 (third column). NASA Energy and Water-cycle Study (NEWS, L'Ecuyer et al. 2015, Stephens and L'Ecuyer 2015; fourth and fifth columns) provide data using objective constraints on the turbulent fluxes. Hartmann (2016) offers global radiative and non-radiative flux energy balance in its Fig. 2.4 (sixth column). These investigations give energy flow components only for all-sky conditions. The IPCC Assessment Report Six (hereafter AR6, Forster et al. 2021) represents both the all-sky and the cloud-free cases (AR6, Wild et al. 2015, 2018, seventh column). WCRP Global Energy and Water Exchange (GEWEX) program (eighth column) is an ongoing study (Stephens et al. 2023), producing 30 years of data.

Table 1: Data sources of this study. Annual global mean fluxes in Wm^{-2}.

	Stevens & Schwartz (2012)	EBAF Ed2.8	EBAF Ed4.1	L'Ecuyer et al. (2015)	Stephens & L'Ecuyer (2015)	Hartmann (2016)	AR6 (2021)	GEWEX (2023)
All-sky								
TOA								
SW in	340	339.87	340.02	340	340	340	340	340.2
SW up	100	99.62	98.98	102	100	100	100	100.2
LW up	239	239.60	240.24	238	240	239	239	239.5
Surface								
SW down		186.47	186.83	186	185	185	185	184.0
SW up		24.13	23.17	22	22	25	25	23.3
SW net	162	162.34	163.66	164	163	160	160	160.7
LW down	342	345.15	345.04	341	344	345	342	345.1
LW up	397	398.27	398.73	399	399	396	398	400.7
LW net	-55	-53.12	-53.69	-58	-55	-51	-56	-55.6
SW+LW net	107	109.22	109.97	107	108	109	104	105.1
Sensible heat	20			25	26	20	21	25.4
Evaporation	86			81	82	88	82	81.1
Clear-sky								
TOA								
SW in		339.87	340.02				340	
SW up		52.50	53.72				53	
LW up		265.59	266.01				267	
Surface								
SW down		244.06	240.86				247	
SW up		29.74	29.08				33	
SW net		214.32	211.78				214	
LW down		316.27	317.41				314	
LW up		398.40	398.51				398	
LW net		-82.13	-81.1				-84	
SW+LW net		132.19	130.68				130	

https://doi.org/10.5194/egusphere-2023-698
Preprint. Discussion started: 18 April 2023

3 Equations

Looking at the data, we realized that there are long-known equations in the literature that are satisfied by the given data: the two-stream approximation of Schwarzschild's equation, described in his original paper (Schwarzschild 1906, Eq. 11), which is an early solution to the general radiative transfer problem by Schwarzschild (1914).

Schwarzschild's equation (1906, Eq. 11) consists of three terms. At a given level of the atmosphere, the black-body emission E of the layer, the radiative energy A which is transmitted outward at the given layer, and the radiative energy B which is transmitted downward at that layer, may be expressed as a function of A_0 which is the observed outward radiation at the top of the atmosphere, and the optical depth, τ:

$$E = A_0(1 + \tau)/2, \qquad A = A_0(2 + \tau)/2, \qquad B = A_0\,\tau/2 \qquad \text{Schwarzschild (1906, Eq.11)}$$

Milne (1930) mentions that these relationships may be derived from first principles. Applying the theory for the Earth's atmosphere by introducing a black-radiating surface at the lower boundary (the surface of Earth), Emden (1913) realized that there is a discontinuity in the Planck-function at the lower boundary, expressed by the term $A - E = A_0/2$, implying a discontinuity between the temperature of the surface and the temperature of the lowest atmospheric layer, but in the same sentence noted that this discontinuity is greatly diminished by the evaporation of water and convection. We choose this relationship (historical considerations see in the Discussion) as the first equation of our model:

$$A - E = A_0/2 \qquad \text{(I)}$$

Here A is the total (shortwave and longwave) energy absorbed by the surface and also the total energy (upward longwave radiation and convection, i.e., the sum of latent heat, LH, and sensible heat, SH) emitted by the surface, if there is no energy imbalance at the surface. The term E expresses surface upward longwave radiation. The equation connects the surface net SW + LW radiation, that is, SH + LH, to half of the outgoing longwave radiation at the top of the atmosphere, independently of the optical depth. Since in the original logic of deduction for the Sun's atmosphere evidently no clouds were considered, we regard this equation for the clear-sky. CERES EBAF Edition 2.8 data (Rose et al. 2017) satisfy the equation in the clear-sky annual global mean: 530.59 – 398.40 = 265.59/2 with a difference of 0.60 Wm^{-2}.

We are going to control it in the global mean on observed data sets such as the CERES EBAF Edition 4.1 data product, available recently for 22 years from 2000 April to 2022 March.

The second term in Schwarzschild's Eq. (11) describes the total energy absorption and emission of the lower boundary (the Earth's surface), as a function of the outgoing longwave radiation at the upper boundary (the TOA), and of the optical depth at the surface, which is the function of the greenhouse gas absorptions. We tried the equation with several optical depth values, and found that most of the observed data sets are satisfied with the choice of $\tau = 2$. Therefore, the second equation of our model will be, still for clear-sky conditions:

https://doi.org/10.5194/egusphere-2023-698
Preprint. Discussion started: 18 April 2023

$$A = 2A_0 \quad \text{(II)}$$

With the CERES EBAF Ed2.8 (Rose et al. 2017) data, Eq. (II) is satisfied as 530.59 = 2 × 265.59 with a difference of -0.59 Wm^{-2}.

All-sky versions of these two equations can easily be created by separating atmospheric radiation transfer from the longwave cloud radiative effect (LWCRE). Our third equation therefore will be the same as Eq. (I),

$$A - E = (A_0 - L)/2 \quad \text{(III)}$$

with all-sky values in the left-hand side, all-sky A_0 (OLR) on the right-hand side, and L stands here for LWCRE.
Our fourth equation is formed from Eq. (II), again with all-sky value at the surface in A and at the TOA in A_0 (i.e., in OLR), and adding the longwave cloud effect:

$$A = 2A_0 + L \quad \text{(IV)}$$

To compare to observed data, we write them in the CERES notation. Let be Surface SW net = Surface (SW down – SW up); Surface LW net = Surface (LW down – LW up) and TOA LW = OLR, then

Surface (SW net + LW net) (clear-sky) = OLR(clear-sky) / 2 (1)
Surface (SW net + LW down) (clear-sky) = 2OLR(clear-sky) (2)
Surface (SW net + LW net) (all-sky) = [OLR(all-sky) – LWCRE] / 2 (3)
Surface (SW net + LW down) (all-sky) = 2OLR(all-sky) + LWCRE (4)

If there is equilibrium at the surface, the absorbed and emitted energy are equal. With the SH and LH components of the convective fluxes, the equations look like:

Surface SH + LH (clear-sky) = OLR(clear-sky) / 2 (1a)
Surface LW up + SH + LH (clear-sky) = 2OLR(clear-sky) (2a)
Surface SH + LH (all-sky) = [OLR(all-sky) – LWCRE] / 2 (3a)
Surface LW up + SH +LH (all-sky) = 2OLR(all-sky) + LWCRE (4a)

https://doi.org/10.5194/egusphere-2023-698
Preprint. Discussion started: 18 April 2023

These theoretical equations do not separate absorbed solar radiation (ASR) into its incoming and reflected components, neither at TOA, nor at the surface. Solar reflection and absorption will be investigated on observational grounds, both for all-sky and clear-sky conditions, in the "Discussion: Empirical extension" sub-session.

4 Results: validation of the equations

4.1 Stevens and Schwartz (2012)

Stevens and Schwartz (2012, Table 1) gave an estimate of Earth's global mean energy flow system based on observation and simulations, with the following all-sky data: Latent heat flux = 86, Sensible heat flux = 20, OLR = 239, and calling LWCRE from CERES as 26.5 Wm^{-2}; the all-sky net equation (3a) looks like 86 + 20 = 106 = (239 – 26.5)/2, the difference is 0.25 Wm^{-2}. For the all-sky total energy equation (4a), including surface upward emission, 397 + 106 = 2 × 239 + 26; the difference is –1 Wm^{-2}.

4.2 NASA Energy and Water-cycle Study (L'Ecuyer et al. 2015)

This study aims to apply balance constraints on energy and water cycles, since in contemporary flux datasets surface net radiation exceeds the corresponding turbulent heat fluxes by 13-24 Wm^{-2}. Based on regional assessments of the components of the hydrological cycle (evaporation, precipitation and runoff), their best estimate of the net radiation at the surface (and therefore the sum of the sensible heat and latent heat flux) globally is 106 Wm^{-2}, which can be regarded as the most accurate estimate. The assessment is constrained only to all-sky conditions. Since longwave cloud effect is not indicated, we took it from the L'Ecuyer et al. (2019) as the mean LWCRE = 26.7 Wm^{-2}.

SFC (SW net + LW net) (all-sky) = SH + LH = [OLR(all-sky) – LWCRE]/2			(3a)
164 – 58 = 25 + 81 = (238 – 26.7)/2	**+ 0.35**	L'Ecuyer et al.	(4a)
SFC (SW net + LW down) (all-sky) = ULW + SH +LH (all-sky) = 2OLR(all-sky) + LWCRE		L'Ecuyer et al.	
164 + 341 = 399 + 25 + 81 = 2 × 238 + 26.7	**+ 2.3**		

The difference in the net, clear-sky equation (1) is only 0.35 Wm^{-2}, less than the indicated Net Absorption at the surface, 0.45 ± 0.4 Wm^{-2}. The noted uncertainty in the sensible heat (25 Wm^{-2}) and latent heat (evaporation) (81 Wm^{-2}) components are ± 4 Wm^{-2}. The mean bias of the two all-sky equations together is 1.32 Wm^{-2}.

https://doi.org/10.5194/egusphere-2023-698
Preprint. Discussion started: 18 April 2023

4.3 Stephens and L'Ecuyer (2015)

In an update to L'Ecuyer et al. (2015), Stephens and L'Ecuyer (2015) (see again our Figure 5 in the Introduction) provided a second optimization where the TOA fluxes are more tightly constrained to CERES EBAF fluxes. OLR and DLR have been increased, and, as a result, turbulent fluxes become 108 Wm^{-2} (with SH = 26 Wm^{-2}, LH (evaporation) = 82 Wm^{-2}); with the accuracy of Eq. (3a) as 1.35 Wm^{-2} and of Eq. (4a) as 0.3 Wm^{-2}; altogether the mean bias of Eq. (3a) and Eq. (4a) has decreased to 0.82 Wm^{-2}.

SFC (SW net + LW net) (all-sky) = SH + LH = [OLR(all-sky) – LWCRE]/2			(3a) St & L'E
163 – 55 = 26 + 82 = (240 – 26.7)/2	**+ 1.35**		
SFC (SW net + LW down) (all-sky) = ULW + SH +LH (all-sky) = 2OLR(all-sky) + LWCRE			(4a) St & L'E
163 + 344 = 399 + 26 + 82 = 2 × 240 + 26.7	**+ 0.3**		

4.4 Hartmann (2016)

Hartmann (2016) has the following values (data from its Fig. 2.4, LWCRE = 26 Wm^{-2} from its Table 3.2):

Thermals + Latent heat = (OLR – LWCRE) / 2			(3a)
20 + 88 = (239 – 26)/2	**+ 1.5**		Hartmann
Thermals + Latent heat + IR emission from surface = 2OLR + LWCRE			(4a)
20 + 88 + 396 = 2 × 239 + 26			Hartmann

Eq. (3a) is valid with a difference of 1.5 Wm^{-2}; Eq. (4a) is exact.

4.5 CERES EBAF Edition 2.8

At the time our recent study has started, the best satellite-based data product was CERES EBAF Edition 2.8, spanning over 16 years (from March 2000 to February 2016). The accuracy of Eq. (1) is 0.60 Wm^{-2}, with the immediate consequence of connecting surface net radiation unequivocally to half of the outgoing TOA LW radiation in the clear-sky. The estimated heat uptake of Earth in that time was the same, 0.58±0.38 Wm^{-2} (Loeb et al. 2012). The same accuracy of Eq. (2), 0.59 Wm^{-2} is a strong verification of the choice of $\tau = 2$. Let us emphasize again that this accuracy of Eq. (2) is not a theoretical expectation but an unforeseen observation. Bias of the all-sky equations (2.4 Wm^{-2} and 2.3 Wm^{-2}) is half the magnitude of the CERES instrument calibration uncertainty of 4.2 Wm^{-2} or standard CERES net flux of 6.5 Wm^{-2} (Loeb et al. 2009).

https://doi.org/10.5194/egusphere-2023-698
Preprint. Discussion started: 18 April 2023

SFC (SW net + LW net) (clear-sky)	= OLR(clear-sky) / 2		(1)
214.32 – 82.13	= 265.59/2	**– 0.60**	Ed2.8
SFC (SW net + LW down) (clear-sky)	= 2OLR(clear-sky)		(2)
214.32 + 316.27	= 2 × 265.59	**– 0.59**	Ed2.8
SFC (SW net + LW net) (all-sky)	= [OLR(all-sky) – LWCRE] / 2		(3)
162.34 – 53.12	= (239.60 – 25.99)/2	**+ 2.41**	Ed2.8
SFC (SW net + LW down) (all-sky)	= 2OLR(all-sky) + LWCRE		(4)
162.34 + 345.15	= 2 × 239.60 + 25.99	**+ 2.30**	Ed2.8

4.6 CERES EBAF Edition 4.1 & 4.2

Using this data product on the full available EBAF data (22 running years from April 2000 through March 2022; 264 monthly means), the mean bias of the four equations together is 0.0007 Wm^{-2}. Below we indicate the most recently released EBAF Edition 4.2 data for the same time period as well.

SFC (SW down – SW up + LW down – LW up) (clear) = OLR (clear) / 2		**Difference**	(1)
240.8680 – 29.0724 + 317.4049 – 398.5211	= 266.0122 /2	–2.3267	Ed4.1
241.1519 – 29.7397 + 317.8570 – 398.6099	= 266.1348 /2	–2.4081	Ed4.2
SFC (SW down – SW up + LW down) (clear) = 2OLR (clear)			(2)
240.8680 – 29.0724 + 317.4049	= 2 × 266.0122	–2.8238	Ed4.1
241.1519 – 29.7397 + 317.8570	= 2 × 266.1348	–3.0005	Ed4.2
SFC (SW down – SW up + LW down – LW up) (all) = [OLR (all) – LWCRE] /2			(3)
186.8544 – 23.1629 + 345.0108 – 398.7550	= (240.2450 – 25.7671)/2	+2.7083	Ed4.1
187.0918 – 23.4436 + 346.1147 – 398.4220	= (240.3317 – 25.8032)/2	+4.0766	Ed4.2
SFC (SW down – SW up + LW down) (all) = 2OLR (all) + LWCRE			(4)
186.8544 – 23.1629 + 345.0108	= 2 × 240.2450 + 25.7671	+2.4450	Ed4.1
187.0918 – 23.4436 + 346.1147	= 2 × 240.3317 + 25.8032	+3.2963	Ed4.2
Mean bias		0.0007	Ed4.1
		0.4911	Ed4.2

https://doi.org/10.5194/egusphere-2023-698
Preprint. Discussion started: 18 April 2023

4.7 IPCC AR6 (2021)

Surface (SW net + LW net) (clear-sky)	= OLR(clear-sky) / 2		(1)
214 – 84	= 267/**2**	**–3.5**	AR6
Surface (SW net + LW down) (clear-sky)	= 2OLR(clear-sky)		(2)
214 + 314	= 2 × 267	**– 6**	AR6
Surface (SW net + LW net) (all-sky)	= [OLR(all-sky) – LWCRE] / 2		(3)
160 – 56	= (239 – 28) /2	**– 1.5**	AR6
Surface (SW net + LW down) (all-sky)	= 2OLR(all-sky) + LWCRE		(4)
160 + 342	= 2 × 239 + 28	**– 4**	AR6

The largest differences on the whole dataset (-6 Wm^{-2} and -4 Wm^{-2}) appear here in Eq. (2) and Eq. (4), mainly caused by the low value attached to downward longwave radiation in this estimate (314 Wm^{-2} in the clear-sky and 342 Wm^{-2} in the all-sky). As mentioned, the most recent data by CERES gives 317.86 Wm^{-2} in the clear-sky and 346.1 Wm^{-2} in the all-sky. Wild (2020) updates the AR6 data by finding higher values in climate models like CMIP6 for this flux component: 318 Wm^{-2} in the clear-sky and 344 Wm^{-2} in all-sky, decreasing the difference of both the equations to -2 Wm^{-2}.

4.8 GEWEX (Stephens et al. 2023)

Sensible heat + Evaporation = (OLR – LWCRE) / 2	(3a)
25.4 + 81.1 = (239.5 – 26.7)/2 **+ 0.1**	GEWEX
Surface (SW net + LW down) = 2OLR + LWCRE	(4)
160.7 + 345.1 = 2 × 239.5 + 26.7 **+ 0.1**	GEWEX

This quantification is based on 30 years of up-to-date GEWEX data products (Stephens et al. 2023). Since neither clear-sky data nor cloud effects are indicated, we take the LWCRE from the study of L'Ecuyer et al. (2019) [27.1 Wm^{-2} at TOA and 26.3 Wm^{-2} at the surface] with a mean value of 26.7 Wm^{-2}. Both all-sky equations are valid with a difference of 0.1 Wm^{-2}, see Figure 8.

Note that with the data in the diagram, radiative heating of the surface, as described by equation (4) [160.7 + 345.1 = 505.8 Wm^{-2}] is less than radiative + non-radiative cooling, represented by equation (4a) [400.7 + 25.4 + 81.1 = 507.2 Wm^{-2}], indicating a negative EEI of -1.4 Wm^{-2} at the surface, in contrast to the stated positive EEI of 0.54 Wm^{-2} at TOA.

https://doi.org/10.5194/egusphere-2023-698
Preprint. Discussion started: 18 April 2023

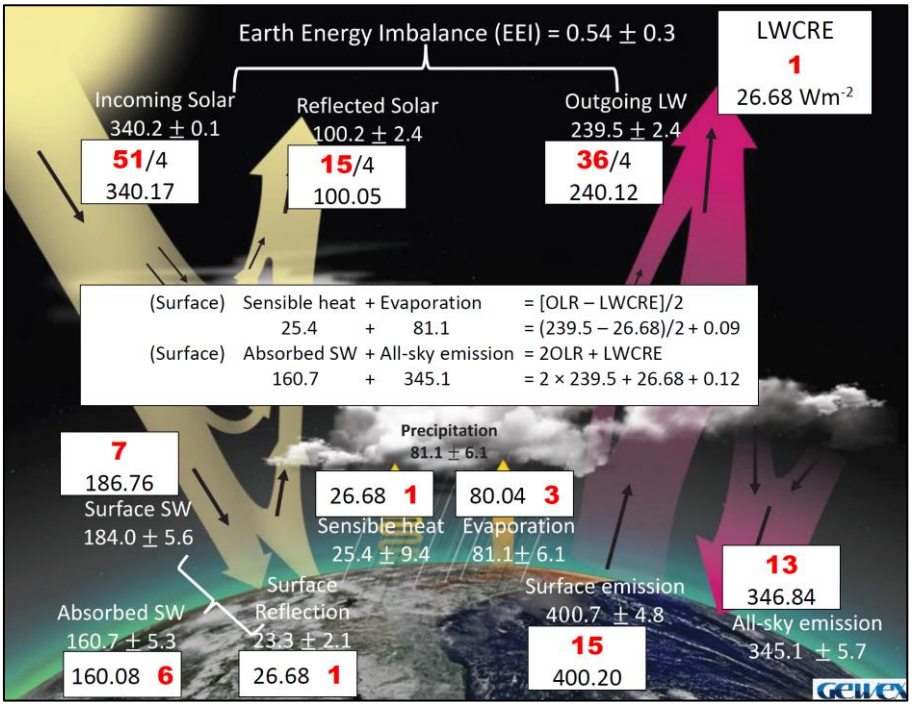

Figure 8: The integer solution of the four equations projected on the updated GEWEX study (Figure SB3 of Stephens et al. 2023). The largest difference at TOA is 0.62 Wm^{-2} (OLR); at the surface 3.38 Wm^{-2} (Surface SW Reflection). Notice that Incoming Solar Radiation and Reflected Solar Radiation at TOA differs from the theoretical integer position with 0.03 Wm^{-2} and 0.15 Wm^{-2}, respectively. The all-sky equations are satisfied within 0.09 Wm^{-2} and 0.12 Wm^{-2}. There is a negative -1.4 Wm^{-2} EEI at the surface.

5 Discussion

5.1 Eq. (1) in historical perspective

Eq. (I) is referred to in standard atmospheric textbooks like Goody (1964, Eq. 2.115), Houghton (1977, Eq. 2.13) or Goody and Yung (1989, Eq. 2.146), and graphically represented for example in Chamberlain (1978, Fig. 1.4) or Hartmann (1994, Fig. 3.11). Manabe and Strickler (1964, Fig. 4) and Manabe and Wetherald (1967, Fig 5.) correctly reproduce the size of discontinuity (also quoted and re-calculated by Hartmann 1994, 2016, Fig. 3.16), but do not utilize the equation as a constraint on its magnitude. Hartmann (1994, pp. 61-63, Figs. 3.10-3.11) presents a two-layer radiative equilibrium model where the equation is valid with a difference of 0.31 Wm^{-2} [the temperature of the surface is T_S = 335 K, the temperature of the air adjacent to the surface is T_{SA} = 320 K and the effective emission temperature at TOA is T_e = 255 K, hence $\sigma(T_S^4 - T_{SA}^4 - T_e^4/2) = -0.31$ Wm^{-2}].

Let us recall that Stephens et al. (1994) utilize the same model, where Eq. (1a) and (1b) describe simple transfer equations in radiative equilibrium, with a solution in Eq. (5a) and (5b) for the upward and downward hemispheric fluxes:

https://doi.org/10.5194/egusphere-2023-698
Preprint. Discussion started: 18 April 2023

$$F\uparrow(\tau_S) = \sigma T_S^4 = F_\infty (2 + \tau_S)/2 \qquad \text{(Stephens et. al 1994, 5a)}$$

$$F\downarrow(\tau_S) = F_g \quad = F_\infty \tau_S/2 \qquad \text{(Stephens et. al 1994, 5b)}$$

These equations, with $F_0(\tau_S) = \sigma T_0^4 = F_\infty(1 + \tau_S)/2$, are equivalent to the three terms in Schwarzschild's (1906, Eq. 11). Therefore, $\Delta\sigma T_S^4 = \sigma T_S^4 - \sigma T_0^4 = F_\infty/2$, as shown in textbooks (see Figure 9).

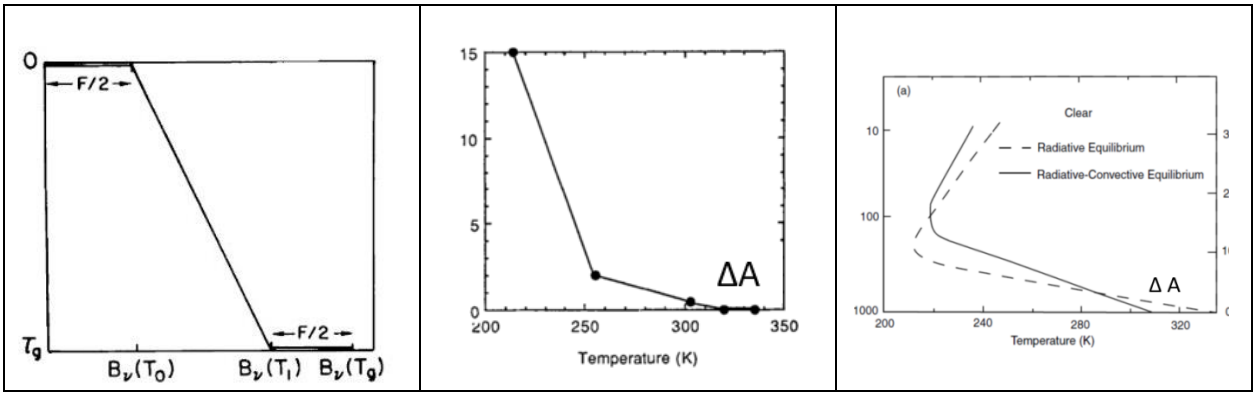

Figure 9: Graphical representations of the discontinuity (net radiation at the surface) in radiative equilibrium; and the corresponding convective flux in radiative-convective equilibrium. Left panel: Chamberlain (1978, Fig. 1.4); middle panel: Hartmann (1994, Fig. 3.11); right panel: Liou (2002, Fig. 8.9)

5.2 Solution to the equations: The integer system

The geometric representation of $A = 2A_0$ given in Figure 10 (after Hartmann 1994, Fig. 2.3).

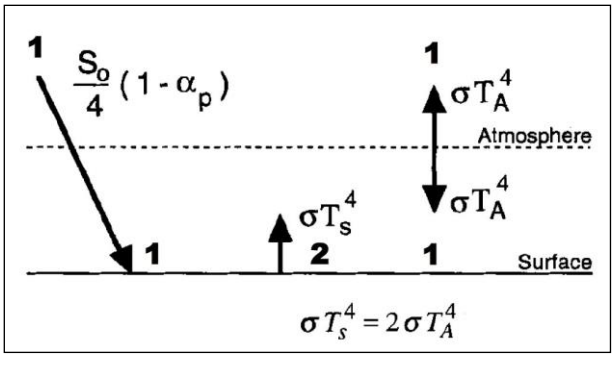

Figure 10: The simplest greenhouse model representing Eq. (2), $A = 2A_0$, in radiative equilibrium. The ratios are indicated. After Hartmann (1994, Fig. 2.3)

https://doi.org/10.5194/egusphere-2023-698
Preprint. Discussion started: 18 April 2023

Improving the model by allowing convective fluxes at the surface according to Eq. (1), A – E = ΔA = $A_0/2$, the model will become as follows as shown in Figure 11:

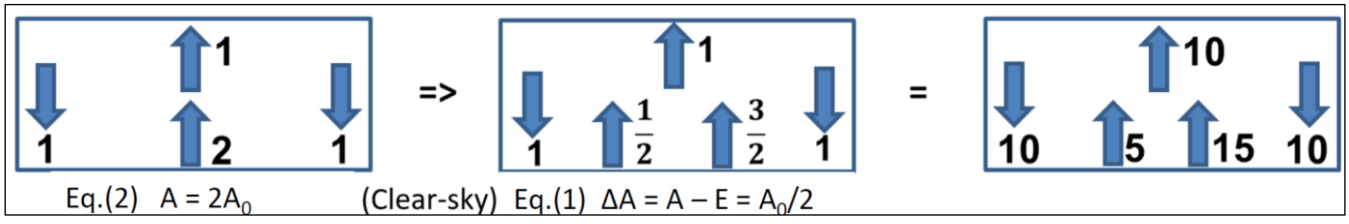

Figure 11: Left, the geometry according to Eq. (2); Middle: including the net radiation at the surface according to Eq. (1) and (2). The right panel is equivalent to the middle, after multiplying the unit by ten.

In radiative equilibrium, ΔA = $A_0/2$ is discontinuity at the surface. In radiative-convective equilibrium, ΔA = $A_0/2$ is the convective flux. Since the unit is not yet specified, as a preparation we multiply it by ten.

Including the all-sky equations (3) and (4) and choosing the longwave cloud radiative effect as the unit: LWCRE = **1** (shown in red bold typeset), we have a geometric solution for the four equations, see Figure 12.

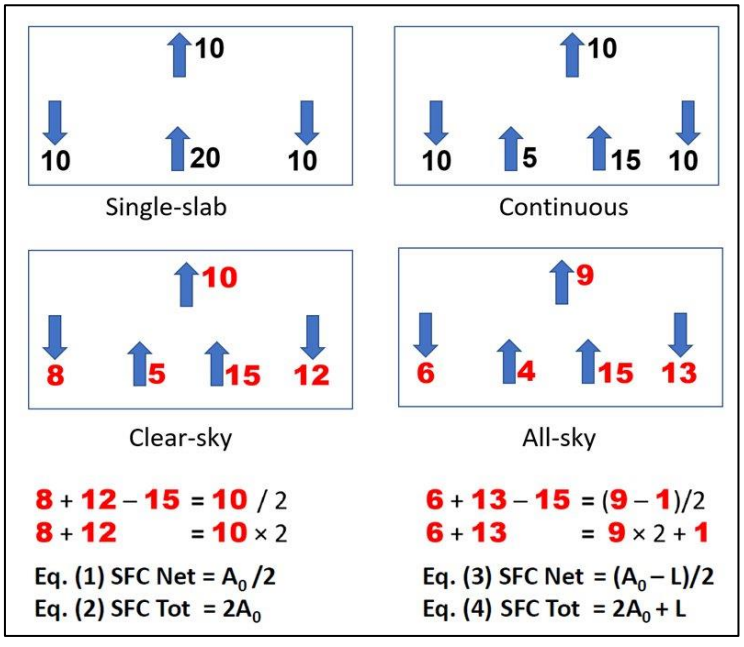

Figure 12: Idealized geometric equilibrium representation of the four equations with integers. No reference to atmospheric gaseous composition was made. Surface fluxes are unequivocally connected to the TOA fluxes. Numbers shown in red are integer multiples of L = LWCRE = 1

The best fit for the unit flux to the CERES data is LWCRE = 1 unit = 26.68 ± 0.02 Wm^{-2}. In Table 2 we present the theoretical fluxes, the CERES fluxes and their differences (Wm^{-2}), including the latest release of EBAF Edition 4.2.

https://doi.org/10.5194/egusphere-2023-698
Preprint. Discussion started: 18 April 2023

Table 2: CERES EBAF Ed4.1 & Ed4.2, 22-yr global means (April 2000 – March 2022). Clear-sky with Δ^C (Loeb et al. 2020). Unit = 26.68 Wm^{-2}.

	Clear-sky	N	N × Unit	Ed4.1	Diff	Ed4.2	Diff
TOA	LW	10	266.80	266.01	-0.79	266.13	-0.67
Surface	SW Net	8	213.44	211.80	-1.64	211.41	-2.03
	LW down	12	320.16	317.40	-2.76	317.86	-2.3
	LW up	15	400.20	398.52	-1.68	398.61	-1.59
	LW Net	-3	-80.04	-81.12	-1.08	-80.75	-0.71
	TOT Net	5	133.40	130.68	-2.72	130.66	-2.74
	All-sky	N	N × Unit	Ed4.1	Diff	Ed4.2	Diff
TOA	LW	9	240.12	240.25	0.13	240.33	0.21
Surface	SW Net	6	160.08	163.69	3.61	163.65	3.57
	LW down	13	346.84	345.01	-1.83	346.11	-0.73
	LW up	15	400.20	398.75	-1.45	398.42	-1.78
	LW Net	-2	-53.36	-53.74	-0.38	-52.31	1.05
	TOT Net	4	106.73	109.95	3.22	111.34	4.61
	CRE	N	N × Unit	Ed4.1	Diff	Ed4.2	Diff
	LW	1	26.68	25.77	-0.91	25.80	-0.88

The largest difference in individual flux components is -2.75 Wm^{-2} in LW down to surface in the clear-sky, and 3.58 Wm^{-2} in the surface solar absorption in the all-sky, still within the stated uncertainties of the CERES fluxes.

5.3 Empirical extension of the integer system

5.3.1 Solar radiation at top of the atmosphere, clear-sky and all-sky

Our equations do not resolve SW radiation into its downward and upward components, neither at TOA, nor at the surface, neither in the clear-sky, nor in the all-sky. As an unexpected observation, these flux components fit into the integer ratio system with remarkably good accuracy.

https://doi.org/10.5194/egusphere-2023-698
Preprint. Discussion started: 18 April 2023

According to the same CERES data product, the global mean clear-sky solar reflection at the top of the atmosphere is 53.72 Wm^{-2}, while the integer position would be **2** units = 53.36 Wm^{-2}. In the all-sky, solar reflection at TOA is 98.98 Wm^{-2}, the corresponding integer ratio is **15**/4 = 100.05 Wm^{-2}. Outgoing longwave radiation position is **9** units. These mean that on the cross-section disk to incoming solar radiation, in all-sky, **15** units are reflected and **36** units of thermal radiation are emitted. These two data together point to an integer position to total solar irradiance as TSI = 51 units, with a value of 51 × 26.68 = 1360.68 Wm^{-2}. As a comparison, the accepted mean value of 17-year SORCE/TIM TSI = 1360.886 Wm^{-2} (Kopp and Lean 2011, Kopp 2021); the difference is 0.21 Wm^{-2}. According to the CERES EBAF Edition 4.1 Version 3 Data Quality Summary, incoming solar radiation in the past two decades was 339.88 Wm^{-2}. Using the geodetic weighting factor of 4.0034, TSI will be 339.88 × 4.0034 = 1360.68 Wm^{-2}.

In clear-sky, on the disk: solar reflection of **8** units and thermal emission of **40** units with TSI = **51** units point to **43** units of absorbed solar radiation and **3** units of TOA net clear-sky imbalance. The corresponding values, after spherical weighting to Earth geometry: ASR(clear-sky) = **43**/4 units = 286.81 Wm^{-2} and the TOA imbalance in the clear-sky) is **3**/4 unit = 20.01 Wm^{-2}. These values in the CERES data are: ASR (clear) = 286.3 Wm^{-2} and, with clear-sky OLR = 266.01 Wm^{-2}, clear-sky TOA net imbalance = 20.29 Wm^{-2}. The accurate fit of the CERES data to the theoretical value derived from the integer position underlines the importance of the possible most accurate knowledge of total solar irradiance.

Having SW reflection at TOA = 15/4 units in the all-sky and incoming solar radiation, ISR = TSI/4 = 51/4 units, we have a prescribed theoretical integer ratio for the all-sky TOA planetary albedo α = 15/51. Its value is 0.294, being arithmetically equivalent to the albedo of IPCC AR6, α = 100/340 (Forster et al. 2021, Figure 7.2); see Table 3.

Table 3: Observed TOA SW integer positions. TSI = 1360.68 Wm^{-2}. Unit = 26.68 Wm^{-2}.

TSI = **51**	Clear-sky	**N**	**N** × Unit	Ed4.1	Diff	Ed4.2	Diff
TOA	SW in	**51**/4	340.17	340.02	-0.15	340.18	0.01
	SW up	**8**/4	53.36	53.72	0.36	53.76	0.40
	LW up	**40**/4	266.80	266.01	-0.79	266.13	-0.67
	Net	**3**/4	20.01	20.29	0.28	20.29	0.28
	All-sky	**N**	**N** × Unit	Ed4.1	Diff	Ed4.2	Diff
TOA	SW in	**51**/4	340.17	340.02	-0.15	340.18	0.01
	SW up	**15**/4	100.05	98.96	-1.09	99.05	-1.00
	LW up	**36**/4	240.12	240.25	0.13	240.33	0.21
	Net	0	0	0.81	0.81	0.80	0.80
CRE	SW	-**7**/4	-46.69	-45.24	1.45	-45.28	1.41
	LW	**1**	26.68	25.77	-0.91	25.80	-0.88
	Net	-**3**/4	-20.01	-19.48	0.53	-19.48	0.53

https://doi.org/10.5194/egusphere-2023-698
Preprint. Discussion started: 18 April 2023

5.3.2 Sensible heat (SH) and latent heat (LH)

Convective fluxes at the surface are not separated in the equations into their sensible heat and evaporation components either. However, the most reliable global mean energy and water cycle-study of NASA (L'Ecuyer et al. 2015) offers SH = 25 ± 4 Wm^{-2} and latent heat as evaporation, E = 81 ± 4 Wm^{-2}; the GEWEX study (Stephens et al. 2023) gives 25.4 ± 9.4 Wm^{-2} and 81.1 ± 6.1 Wm^{-2} (see our Table 1), while the corresponding integer positions are 1 unit = 26.68 Wm^{-2} and 3 units = 80.04 Wm^{-2}. The accurate fit of convection and evaporation into the integer system is one of the most far-reaching results of this investigation. It seems that not only their sum is constrained unequivocally to (OLR – LWCRE)/2 as Eq. (3a) prescribes, but the two non-radiative components in the hydrological cycle follow individually the confinement to the integer structure, posing strict stability criteria for water vapor feedback theories — and calling theoretical explanation itself.

6 Conclusions

— Integer ratios were observed in several global mean energy flow estimates. To demonstrate their reality and provide physical basis of the relationships, four radiative transfer equations were presented; each is a version of the original plane-parallel model of Schwarzschild. Contrary to several limitations of that model, the accuracy of the equations on well-established data products suggests that Earth's system dynamics follows these simplest radiative transfer constraint equations.

— We presented a solution to the equations, describing surface energy flows related to observed TOA fluxes and provided a geometric representation for them. An unexpected implication of this solution is the possibility to extend it to flux components that are not involved in the original four equations. All the flux values appear to be close to their integer position within the stated range of uncertainty.

—There are several limitations and unknowns in this model. While the global mean integer flow system can be expressed as the solution of the simplest two-stream approximation of the original Schwarzschild equations, it is not clear why this elementary physical radiation transfer model, and the corresponding single-layer atmospheric geometry is satisfied with such a high accuracy in the observed data.

— The same annual global mean state can be implemented through several different regional, local, vertical and seasonal distributions, therefore, while the mean state may be maintained under changing atmospheric gaseous composition, all the geographic and inter-annual climatic states may undergo forced variation.

— The limits of the stability constraints are not known, the magnitude of fluctuations around, or the systematic deviation from the equilibrium position is an open question. The behaviour of the structure during climatic shifts and glaciations is yet unknown.

Competing interests. The author declares no conflict of interest.

https://doi.org/10.5194/egusphere-2023-698
Preprint. Discussion started: 18 April 2023

References

CERES_EBAF_Ed4.1 Data Quality Summary Version 3, 12/9/2021, https://ceres.larc.nasa.gov

Chamberlain, J.W.: Theory of planetary atmospheres, Academic Press, New York, London, 1978

Emden, R.: Über Strahlungsgleichgewicht und atmosphärische Strahlung. Sitzungsberichte der mathematisch-physicalischen Klasse der K.B. Akademie der Wissenschaften, München, 43, 55-142, 1913.

Forster, P., T. Storelvmo, K. Armour, W. Collins, J.-L. Dufresne, D. Frame, D.J. Lunt, T. Mauritsen, M.D. Palmer, M. Watanabe, M. Wild, and H. Zhang: The Earth's Energy Budget, Climate Feedbacks, and Climate Sensitivity. In Climate Change 2021: The Physical Science Basis. Contribution of Working Group I to the Sixth Assessment Report of the Intergovernmental Panel on Climate Change [Masson-Delmotte, V., P. Zhai, A. Pirani, S.L. Connors, C. Péan, S. Berger, N. Caud, Y. Chen, L. Goldfarb, M.I. Gomis, M. Huang, K. Leitzell, E. Lonnoy, J.B.R. Matthews, T.K. Maycock, T. Waterfield, O. Yelekçi, R. Yu, and B. Zhou (eds.)]. Cambridge University Press, Cambridge, United Kingdom and New York, NY, USA, pp. 923–1054, doi:10.1017/9781009157896.009, 2021.

Goody, R. M.: Atmospheric Radiation I: Theoretical Basis. Oxford Univ. Press, London, 1964.

Goody, R.M. and Yung, Y.L.: Atmospheric Radiation I: Theoretical Basis, 2nd Ed. Oxford Univ. Press, London, 1989

Hartmann, D.: Global physical climatology. Academic Press, San Diego, New York, 1994

Houghton, J.: The physics of atmospheres. Cambridge Univ Press, 1977

Kato, S., Fred G. Rose, David A. Rutan, Tyler J. Thorsen, Norman G. Loeb, David R. Doelling, Xianglei Huang, William L Smith, Wenying Su and Seung-Hee Ham : Surface Irradiances of Edition 4.0 Clouds and the Earth's Radiant Energy System (CERES) Energy Balanced and Filled (EBAF) Data Product. J. Climate, 31, 4501–4527, https://doi.org/10.1175/JCLI-D-17-0523.1, 2018

Kiehl, J. and Trenberth, K.: Earth's annual global mean energy budget. Bull Am Met Soc 78, 2, 197-208, 1997.

Kopp, G. and Lean, J.: A new, lower value of total solar irradiance Geophys. Res. Lett., 38, L01706, 2011.

Kopp, G. 2021: Science Highlights and Final Updates from 17 Years of Total Solar Irradiance Measurements from the SOlar Radiation and Climate Experiment/Total Irradiance Monitor (SORCE/TIM). Solar Physics (2021)296:133

L'Ecuyer, T.S., H. K. Beaudoing, M. Rodell, W. Olson, B. Lin, S. Kato, C. A. Clayson, E. Wood, J. Sheffield, R. Adler, G. Huffman, M. Bosilovich, G. Gu,, F. Robertson, P. R. Houser, D. Chambers, J. S. Famiglietti, E. Fetzer, W. T. Liu, X. Gao, C. A. Schlosser, E. Clark, D. P. Lettenmaier, and K. Hilburn: The Observed State of the Energy Budget in the Early Twenty-First Century. J. Climate, 28, 8319-8346, 2015.

L'Ecuyer, T., Y. Hang, A. V. Matus and Z. Wang: Reassessing the Effect of Cloud Type on Earth's Energy Balance in the Age of Active Spaceborne Observations. Part I: Top of Atmosphere and Surface. J. Climate, 32:6197-6217, 2019.

Liou, K-N.: An introduction to atmospheric radiation, Second edition. Academic Press, New York, London, 2002.

Loeb, N. G., B. A. Wielicki, D. R. Doelling, G. L. Smith, D. F. Keyes, S. Kato, N. Manalo-Smith, and T. Wong: Toward Optimal Closure of the Earth's Top-of-Atmosphere Radiation Budget. Journal of Climate, 22, 3, 748-766, 2009.

https://doi.org/10.5194/egusphere-2023-698
Preprint. Discussion started: 18 April 2023

Loeb, N. G., J. M. Lyman, G. C. Johnson, R. P. Allan, D. R. Doelling, T. Wong, B. J. Soden and G. L. Stephen: Observed changes in top-of-the-atmosphere radiation and upper-ocean heating consistent within uncertainty. Nature Geoscience, 5(2), 110-113, 2012

Loeb, N. G.: The Recent Pause in Global Warming. Langley Colloquium Series Lecture, 2014.

Loeb, N. G., D. R. Doelling, H. Wang, W. Su, C. Nguyen, J. G. Corbett, L. Liang, C. Mitrescu, F. G. Rose, and S. Kato: Clouds and the Earth's Radiant Energy System (CERES) Energy Balanced and Filled (EBAF) Top-of-Atmosphere (TOA) Edition 4.0 Data Product. J. Climate, 31(2), 895–918, 2018.

Loeb, N. G., F. G. Rose, S. Kato, D. A. Rutan, W. Su, H. Wang, D. R. Doelling, W. L. Smith, and A. Gettelman: Toward a Consistent Definition of Clear-Sky Radiative Fluxes. J. Climate, 33(1), 61-75, 2020.

Manabe, S, and R. F. Strickler: Thermal equilibrium of the atmosphere with a convective adjustment. J. Atmos. Sci., 21, 361–385, 1964.

Manabe, S. and R. T. Wetherald: Thermal Equilibrium of the Atmosphere with a Given Distribution of Relative Humidity. Journal of Atmospheric Sciences 24, 241-259, 1967

Milne, E. A.: Thermodynamics of the stars. Handbuch der Astrophysik, 3, 1930.

Rose, F., S. Kato, N. Loeb, D. Doelling, T. Thorsen and D. Rutan: Ed4 SURFACE_EBAF Part1 Algorithm and Flux Differences from Ed2.8, May 16, CERES Science Team Meeting, 2017

Schwarzschild, K: On the equilibrium of the sun's atmosphere. Nach. K. Gesell, Wiss. Göttingen, Math-Phys. Klasse **195,** 41–53, 1906. In Selected Papers on the Transfer of Radiation (D. H. Menzel, ed.). Dover, New York, 1966.

Schwarzschild, K.: Über Diffusion und Absorption in der Sonnenatmosphäre. Sitzungsberichte der Königlich Preussischen Akademie der Wissenschaften. pp. 1183-1200. In Selected Papers on the Transfer of Radiation (D. H. Menzel, ed.). Dover, New York, 1914.

Stephens, G. L. and T. L'Ecuyer: The Earth's energy balance, Atm Res, 166, 195-203, 2015.

Stephens, G. L., A. Slingo, M. J. Webb, P. J. Minnett, P. H. Daum, L. Kleinman, I. Wittmeyer, and D. A. Randall: Observations of the Earth's Radiation Budget in relation to atmospheric hydrology. 4. Atmospheric column radiative cooling over the world's oceans. Journal of Geographic Research, 99, D9, 18,585-18,604, 1994.

Stephens, G. L., J. Li, M. Wild, C. A. Clayson, N. Loeb, S. Kato, T. L'Ecuyer, P. W. Stackhouse Jr, M. Lebsock, and T. Andrews: An update on Earth's energy balance, Nat Geosci, 5, 691-696., 2012

Stephens, G. L., J. Polcher, X. Zeng, P. van Oevelen, G. Poveda, M. Bosilovich, M-H. Ahn, G. Balsamo, Q. Duan, G. Hegerl, Ch. Jakob, B. Lamptey, R. Leung, M. Piles, Z. Su, P. Dirmeyer, K. L. Findell, A. Verhoef, M. Ek, T. L'Ecuyer, R. Roca, A. Nazemi, F. Dominguez, D. Klocke and S Bony The first 30 years of GEWEX. Bull. Amer. Meteor. Soc., 104 (1), E126-E157, 2023.

Stevens, B. and Schwartz, S.: Observing and Modeling Earth Energy flows. Surv Geophys 33, 779-816, 2012.

Trenberth K. and J. Kiehl, J. Fasullo: Earth's global energy budget. Bull Am Met Soc, 2009 March, 311-324, 2009.

https://doi.org/10.5194/egusphere-2023-698
Preprint. Discussion started: 18 April 2023

Wielicki, B.A.; Barkstrom, B.R.; Harrison, E.F.; Lee, R.B., III; Smith, G.L. and Cooper, J.E.: Clouds and the Earth's Radiant Energy System (CERES): An earth observing system experiment. Bull. Am. Met. Soc. 77, 853–868, 1996

Wild, M., D. Folini, Ch. Schär, N. G. Loeb, E. G. Dutton and G. König-Langlo: The global energy balance from a surface perspective. Clim Dyn. 40:3107-3134, 2013.

Wild, M., D. Folini, M. Z. Hakuba, Ch. Schär, S. I. Seneviratne, S. Kato, D. Rutan, Ch. Ammann, E. F. Wood and G. König-Langlo: The energy balance over land and oceans. Clim. Dyn. 44(11–12), 3393-3429, 2015.

Wild, M., M. Z. Hakuba, D. Folini, P. Dörig-Ott, Ch. Schär, S. Kato and Ch. N. Long: The cloud-free global energy balance and inferred cloud radiative effects. Clim. Dyn. 52:4787–4812, 2019.

Wild, M.: The global energy balance as represented in CMIP6 climate models. Clim Dyn 55: 553-577, 2020.